Am J Physiol Heart Circ Physiol 288: H280–H286, 2005.
First published September 9, 2004; doi:10.1152/ajpheart.00713.2004.

Prediction and assessment of the time-varying effective pulmonary vein area via cardiac MRI and Doppler echocardiography

Andrew W. Bowman and Sándor J. Kovács

Cardiovascular Biophysics Laboratory and Cardiovascular MR Laboratories, Cardiovascular Division, Washington University School of Medicine, St. Louis, Missouri 63110

Submitted 15 July 2004; accepted in final form 8 September 2004

Bowman, Andrew W., and Sándor J. Kovács. Prediction and assessment of the time-varying effective pulmonary vein area via cardiac MRI and Doppler echocardiography. *Am J Physiol Heart Circ Physiol* 288: H280–H286, 2005. First published September 9, 2004; doi:10.1152/ajpheart.00713.2004.—Accurately estimating left atrial (LA) volume with Doppler echocardiography remains challenging. Using angiography for validation, Marino et al. (Marino P, Prioli AM, Destro G, LoSchiavo I, Golia G, and Zardini P. *Am Heart J* 127: 886–898, 1994) determined LA volume throughout the cardiac cycle by integrating the velocity-time integrals of Doppler transmitral and pulmonary venous flow, assuming constant mitral valve and pulmonary vein areas. However, this LA volume determination method has never been compared with three-dimensional LA volume data from cardiac MRI, the gold standard for cardiac chamber volume measurement. Previously, we determined that the effective mitral valve area is not constant but varies as a function of time. Therefore, we sought to determine whether the effective pulmonary vein area (EPVA) might be time varying as well and also assessed Marino's method for estimating LA volume. We imaged 10 normal subjects using cardiac MRI and concomitant transthoracic Doppler echocardiography. LA and left ventricular (LV) volumes were measured by MRI, transmitral and pulmonary vein flows were measured by Doppler echocardiography, and time dependence was synchronized via the electrocardiogram. LA volume, estimated using Marino's method, was compared with the MRI measurements. Differences were observed, and the discrepancy between the echocardiographic and MRI methods was used to predict EPVA as a function of time. EPVA was also directly measured from short-axis MRI images and was found to be time varying in concordance with predicted values. We conclude that because EPVA and LA volume time dependence are in phase, LA filling in systole and LV filling in diastole are both facilitated. Application to subjects in select pathophysiological states is in progress.

pulmonary vein flow; cardiac imaging; diastolic function; left atrial conduit volume

THE NEED TO ASSESS left atrial (LA) size and function is being further advanced by the realization that LA size is a sensitive and specific index of time-averaged diastolic function (1, 29). As such, its determination necessarily relies on knowledge of the time-dependent LA volume throughout the cardiac cycle (22, 26). Accurate measurements of LA volume remain challenging to obtain via two-dimensional and Doppler echocardiography. Whereas calculations of left ventricular (LV) volume using simplified geometric assumptions have proven fairly reliable, similar assumptions simplifying LA geometry have failed to yield accurate calculations of LA volume due to its complex shape (23).

Circumventing the need to calculate LA volumes directly via geometric assumptions, Marino et al. (20) calculated the LA volume as a function of time via integration of Doppler transmitral and pulmonary venous (PV) flow velocity contours. The conservation of volume for an arbitrarily shaped object of variable volume $V(t)$, containing an incompressible fluid and having an inlet and an outlet, requires that

$$V(t) = V_0 + \int \text{inflow} \cdot \text{area}\, dt - \int \text{outflow} \cdot \text{area}\, dt \quad (1)$$

where V_0 denotes the constant of integration. Specifically, Marino et al. postulated that

$$[LA(t) - LA_{min}] = PVA \int PV_{flow}(t) dt - MVA \int MV_{flow}(t) dt \quad (2)$$

where $LA(t)$ refers to the LA volume as a function of time (t), LA_{min} is the minimum LA volume (at ventricular end diastole), PVA is the (constant) PV area, $PV_{flow}(t)$ is the velocity of blood flow through the pulmonary veins as a function of time, MVA is the (constant) mitral valve area, $MV_{flow}(t)$ is the velocity of blood flow across the mitral valve, and *time* $t = 0$ ms refers to the peak of the ECG QRS complex. Consequently, $\int PV_{flow}(t) dt$ was calculated as the continuous velocity-time integral (VTI) of the Doppler flow profile of the right superior PV, and $\int MV_{flow}(t) dt$ was calculated as the continuous VTI of Doppler transmitral flow. Furthermore, they defined

$$MVA = (\text{stroke volume})/(\text{VTI of transmitral flow}) \quad (3)$$

per their earlier work (19) as well as

$$PVA = (MVA \cdot \text{VTI of transmitral flow})/(\text{VTI of PV flow}) \quad (4)$$

From these echocardiographic measurements, they calculated relative LA volume curves. They scaled these volume curves using a two-dimensional estimate of LA volume at end diastole and compared these resulting LA volume curves with those acquired via biplane cine angiography, with good results (20).

With the recent advances in cardiac MRI, it is now feasible to calculate cardiac chamber volume curves as a function of time, and cardiac MRI has become the gold standard for LA volume determination (3, 4, 16, 23, 30, 31). However, LA volume curves derived by Marino's echocardiographic method have not been compared with LA volumes measured via cardiac MRI.

Address for reprint requests and other correspondence: S. J. Kovács, Cardiovascular Biophysics Laboratory, Washington Univ. Medical Center, Box 8086, 660 S. Euclid Ave., St. Louis, MO 63110 (E-mail: sjk@wuphys.wustl.edu).

The costs of publication of this article were defrayed in part by the payment of page charges. The article must therefore be hereby marked "*advertisement*" in accordance with 18 U.S.C. Section 1734 solely to indicate this fact.

Previously, we evaluated left heart function in young healthy adult volunteers by synchronizing LV and LA volume data (obtained via MRI) with transmitral and PV flow data (obtained from Doppler echocardiography) (4). Our results suggested that the effective MVA (EMVA) was not constant and varied throughout early rapid filling, and this was validated in a subsequent study (2). The synchronization of MRI volume data and echocardiographic flow data also suggested that PVA also varied throughout the cardiac cycle. Specifically, the acceleration portion of the PV D-wave corresponded to a large increase in LV volume (not completely accounted for by the simultaneous decrease in LA volume), yet during the deceleration portion of the D-wave, both LV and LA volumes change substantially less (4). The purpose of the present study was to derive and compare LA volume curves generated by Marino's method to those calculated by cardiac MRI, investigate what the differences between these two LA volume curves predict about effective PVA (EPVA), and use cardiac MRI to measure EPVA as a function of time throughout the cardiac cycle.

METHODS

Cardiac MRI. After appropriate informed consent was obtained according to Washington University Medical Center Human Studies Committee guidelines, 10 normal subjects (5 men and 5 women, average age 23 yr) underwent a complete functional cardiac MRI study and concurrent two-dimensional Doppler echocardiography. The MRI portion of our study has been previously described (2–4). Briefly, for the MRI study, the subjects were scanned with a 1.5-T Philips Gyroscan MRI system (Release 9.0, Philips Medical Systems; Best, The Netherlands). Survey images and standard planes for ventricular four-chamber and short-axis views were obtained. Once determined, high-resolution balanced fast field echo cine-loops of the four-chamber view were obtained during breathholds (duration of ~10 s each). These cine-loops, encompassing the entire cardiac cycle, were divided into 20–27 phases triggered from the ECG R-wave.

The initial four-chamber view was used to plan a short-axis cine-stack protocol of between 18 and 20 slices, 9 mm thick with zero gap, spanning the apex of the ventricles through the superior-posterior wall of the LA. Image slices were obtained during 10-s breathholds/slice, and each cine-loop was divided into 20 cardiac phases triggered from the ECG R-wave, covering the entire cardiac cycle. For the short-axis stack image acquisition, the repetition time, echo time, and flip angle were 4.0 ms, 1.47 ms, and 50°, respectively. In-plane resolution of 1.41 mm was obtained with a field of view of 36 cm and a matrix size of 192 × 256 interpolated to 256 × 256.

Upon completion of the exam, the data were archived to 4.1-GB magnetooptical disks. All image analysis was performed off-line on a remote personal computer using eFilm 1.5.3 (eFilm Medical; Toronto, Ontario, Canada), Paint Shop Pro 7 (Jasc Software; Minnetonka, MN), and Scion Image (Scion; Frederick, MD).

In all subjects, the LV and LA endocardial contours were manually traced in each slice at each phase of the three-dimensional dataset, and the corresponding segmental volume was determined (2–4). For each phase, the segmental volumes of the traces were summed via Simpson's rule and evaluated over the cardiac cycle. Intraobserver variability of MRI segmental volume measurements using this method has been previously reported as <4% (2, 4). In circumstances where precise matching of the R-R interval between MRI data and echocardiographic data was necessary, the final MRI-measured diastasis point was duplicated at a time 150 ms before the end of the R-R interval. The measured end-diastolic value was duplicated at the end of the R-R interval as well.

Doppler echocardiography. Either immediately before or after the cardiac MRI exam, while in the MRI laboratory, clinical echocardiographic images were obtained in all subjects in the left lateral decubitus position by an experienced American Society of Echocardiography-certified sonographer using an Acuson Sequoia (Acuson; Mountain View, CA) echocardiographic imaging system equipped with a 3.5-MHz transducer. The imager recorded and displayed on the image the simultaneous limb lead II of the ECG. The sample volume for transmitral Doppler imaging was placed at the mitral leaflet tips in the apical four-chamber view in accordance with American Society of Echocardiography criteria (25). With the use of Doppler color flow as a guide, the sample volume for PV flow waves was placed 1 cm upstream in the right superior PV. To minimize artifacts due to misalignment between the imaging beam and the flow to the extent possible, transmitral flow and PV flow data were obtained by aligning the scan direction along the color Doppler-generated direction of flow. All echocardiographic data were stored digitally on magnetooptical disk for subsequent off-line analysis using ViewPro (Freeland, LLC; Westfield, IN) and Paint Shop Pro. Baseline filters were set to their lowest settings.

Marino's method for calculating LA volume curve. To generate LA volume curves according the method of Marino et al. (20), one Doppler transmitral flow image and one PV flow image from each subject were selected. The criteria to select the images were that they *1*) were empirically representative of all the transmitral or PV flow images and *2*) had R-R intervals that were as identical as possible. For the transmitral flow image, the Doppler E wave and A wave were selected and fit using model-based image processing, a previously validated technique (11, 12, 18) written in LabView 6 (National Instruments; Austin, TX) to yield a numerical representation of the continuous contour for the E and A wave. For the PV flow image, the contours of the PV S wave, D wave, and AR waves were manually traced in Paint Shop Pro and processed using a similar LabView 6 program to generate a numerical representation of the continuous contour of PV flow. Figure 1 illustrates the numerical representations of the transmitral and PV flow contours for one subject.

The LA volume curve was calculated using *Eq. 2*, where $\int PV_{flow}(t)dt$ and $\int MV_{flow}(t)dt$ were calculated from the image-processed transmitral and PV flow images, MVA was calculated via *Eq. 3* with the stroke volume calculated from the MRI-generated LV volume curve, and PVA was calculated via *Eq. 4*, as previously described (20). This relative LA volume curve was scaled using the end-diastolic LA volume measured via the MRI method.

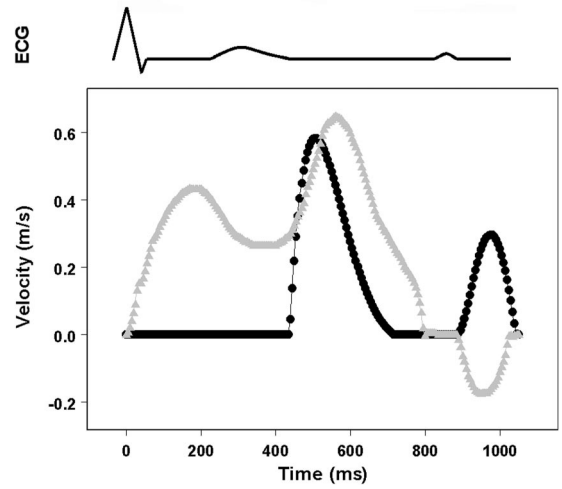

Fig. 1. Numerical representations of Doppler flow profiles for transmitral flow (solid circles) and pulmonary vein flow (shaded triangles) for one normal subject. The ECG displayed is a schematic and serves as an aid to clarify timing within the cardiac cycle. See text for details.

Marino's method for calculating LA volume curve using time-varying EMVA. To evaluate how incorporating the time-varying EMVA as described earlier (2) affected Marino's method for measuring LA volume, the $MVA\int MV_{flow}(t)dt$ term in *Eq. 2* becomes $\int EMVA(t)\cdot MV_{flow}(t)dt$. This term is equivalent to the actual time-dependent volume by which the LV increases during diastole. Therefore, *Eq. 2* transforms into

$$[LA(t) - LA_{min}] = PVA\int PV_{flow}(t)dt - [LV_d(t) - LV_{min}](t) \quad (5)$$

where $LV_d(t)$ is the LV volume as a function of time during diastole only and LV_{min} is the minimum LV volume (at ventricular end systole). Thus $[LV_d(t) - LV_{min}](t)$ represents the net increase in LV volume during diastole. The $[LV_d(t) - LV_{min}](t)$ term was calculated from the MRI LV volume data. To match the temporal resolution of the echocardiographic data [the $PVA\int PV_{flow}(t)dt$ term], the LV volume data from LV_{min} to end diastole were fit with a 10th-order spline using Axum 7 (Mathsoft; Cambridge, MA). The output of the spline fit was incorporated into *Eq. 5*. The $PVA\int PV_{flow}(t)dt$ term remained unchanged from *Eq. 2*.

EPVA prediction. If the EPVA, in addition to the EMVA, is permitted to vary as a function of time, *Eq. 5* may be rewritten as

$$[LA(t) - LA_{min}] = \int EPVA(t)\cdot PV_{flow}(t)dt - [LV_d(t) - LV_{min}](t) \quad (6)$$

where EPVA(t) is the (variable) EPVA as a function of time. Rearranging *Eq. 6* and solving for EPVA(t) by differentiation yields

$$EPVA(t) = (d\{LA(t) + [LV_d(t) - LV_{min}](t)\}/dt)/PV_{flow}(t) \quad (7)$$

To match the temporal resolution of the echocardiographic data [the $PV_{flow}(t)$ term] before sampling, the $LA(t) + [LV_d(t) - LV_{min}](t)$ volume data from MRI was fit with a fifth-order spline using Axum 7 (see Fig. 2), and the output was then differentiated with respect to time and input into *Eq. 7*.

EPVA measurement. To determine the degree to which actual EPVA values mirrored those calculated via *Eq. 7*, the effective areas for all four PVs (combined) were estimated throughout the cardiac cycle in all subjects. With the use of images from the short-axis MRI data in Paint Shop Pro, the width of the orifices of each PV at its insertion to the LA was measured (Fig. 3). Even though PV ostia are known to be elliptical (32), for simplicity, the EPVA for each vein was calculated assuming a circular geometry, with the measured distance acting as the diameter of the vein. The total EPVA was determined in each subject by summing the areas of each vein at each phase of the cardiac cycle. Intraobserver variability was determined using 10 randomly selected images used to measure EPVA; images from all four veins were selected.

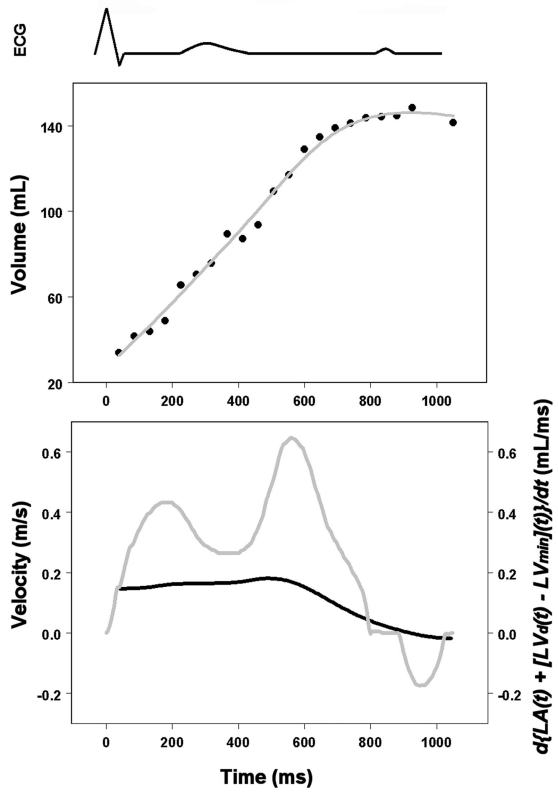

Fig. 2. *A*: plot showing MRI-derived $LA(t) + [LV_d(t) - LV_{min}](t)$ for a single subject (solid circles), where LA(t) refers to the left atrial (LA) volume as a function of time (t), $LV_d(t)$ is the left ventricular (LV) volume as a function of time during diastole only, and LV_{min} is the minimum LV volume (at ventricular end systole). The shaded line is the fifth-order spline curve fit to the data. *B*: the derivative of the spline fit in *A* (i.e., $d\{LA(t) + [LV_d(t) - LV_{min}](t)\}/dt$) is shown in black (using the vertical axis on the *right*), superimposed with the echocardiographic pulmonary vein flow contour from the same subject as described in Fig. 1 (shaded line, using the vertical axis on the *left*). The ratio of the values from the black and shaded lines in *B* yields the predicted effective pulmonary vein area (EPVA) via *Eq. 7*. Note how the derivative of the spline fit is virtually constant until the peak of the pulmonary venous D wave, at which point it decreases as the $LA(t) + [LV_d(t) - LV_{min}](t)$ curve in *A* begins to flatten out. The ECG displayed is a schematic and serves as an aid to clarify timing within the cardiac cycle. See text for details.

RESULTS

LA volume curve comparison. In all subjects, when LA volume curves calculated via Marino's method (*Eq. 2*) and those measured via MRI were compared, the two curves match reasonably well during systole but begin to diverge during diastole (Fig. 4). Specifically, Marino's method consistently (in 9 of 10 subjects) overestimated the amount by which the LA fills during late diastole (by an average of about 15 ml). Incorporation of the time-varying EMVA (*Eq. 5*) yielded varying results. In 9 of 10 subjects, using *Eq. 5* generated a slightly better measure of the late-diastolic LA volume (difference of around 6 ml); however, in one-half of the cases, the early diastolic portions of the calculated volume curve deviated more substantially from the MRI volume curve when the time-varying EMVA was taken into account.

EPVA as a function of time. With the use of *Eq. 7*, the predicted EPVA curve was qualitatively similar in all 10 subjects. Essentially, the curves predict that the EPVA peak near end systole and steadily decrease throughout diastole. When the EPVA was measured using the short-axis MRI data, it was found to be time varying as well (see *animation 1*, http://ajpheart.physiology.org/cgi/content/full/00713.2004.2004/DC1). Specifically, the effective areas for each PV in all subjects varied throughout the cardiac cycle (data from one subject shown in Fig. 5). The areas for each vein followed similar patterns, but different veins often peaked at slightly different times. The overall total EPVA, computed from the summed areas of the four veins, varied throughout the cardiac cycle as well (Fig. 5), in a manner similar to that of the EPVA predicted by *Eq. 7* (Fig. 6). Even though the measured EPVA followed the same trend as the predicted EPVA; however, the calculated EPVA from *Eq. 7* could not precisely predict the exact values for the actual measured EPVA. Intraobserver variability for measured effective pulmonary vein diameters was 7.8% (averaging <1 mm).

To better understand the relationship between EPVA and global LA function, we plotted the Doppler PV flow profile and the measured EMVA curve on similarly scaled axes in all

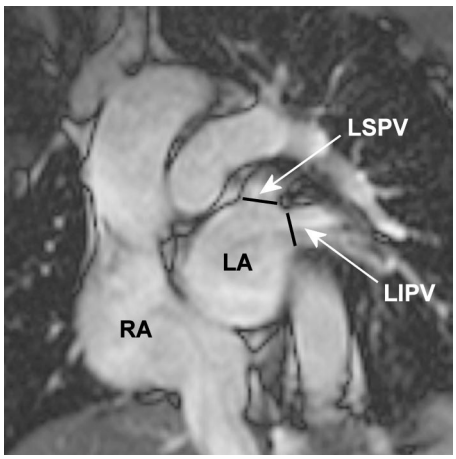

Fig. 3. Measurement of effective pulmonary vein orifice size in the MRI short-axis view of the atria. RA, right atrium; LSPV, left superior pulmonary vein; LIPV, left inferior pulmonary vein. See text for details.

subjects. In 8 of 10 subjects, the EPVA curve peaked near the relative minimum in PV flow at end systole (Fig. 7), when the mitral annulus (and atrial cavity) achieves its most apical displacement. We also plotted the LA volume curve and the measured EPVA curve on similarly scaled axes in all subjects. In 9 of 10 subjects, the EPVA curve, when appropriately scaled, closely followed the LA volume curve (Fig. 8).

DISCUSSION

Even though two-dimensional and Doppler echocardiographies are the most convenient and frequently used methods to evaluate cardiac function and measure chamber size, they have not proven reliable in measuring LA volume precisely. The results demonstrate that Marino's method (20) for calculating the LA volume curve, compared with MRI, yields reliable results during systole but systematically diverges during mid to late diastole. This leads to a meaningful overestimation of the middiastolic expansion volume of the LA and would subsequently lead to overestimation of the LA stroke volume. By synchronizing accurate chamber volume data (from MRI) with transmitral and PV flow data (from echocardiography), we are able to glean new insights into left heart function. In addition to reassessing Marino's method, data

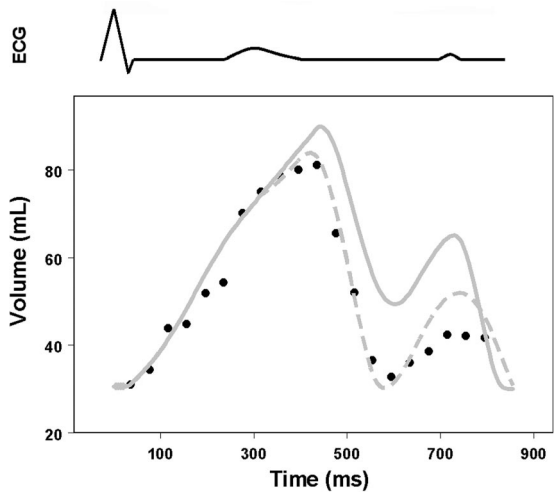

Fig. 4. Plot of echocardiographically predicted versus MRI measured LA volume curves for one subject. The solid circles represent LA volumes measured via MRI. The solid shaded line shows the predicted LA volume curve calculated using Marino's method (*Eq. 2*). The dashed shaded line shows the predicted LA volume curve calculated using Marino's method corrected to account for time-varying effective mitral valve area (*Eq. 5*). Note how both predicted curves overestimate LA volume immediately preceding atrial contraction, although the dashed shaded line demonstrates less error. The ECG displayed is a schematic and serves as an aid to clarify timing within the cardiac cycle. See text for details.

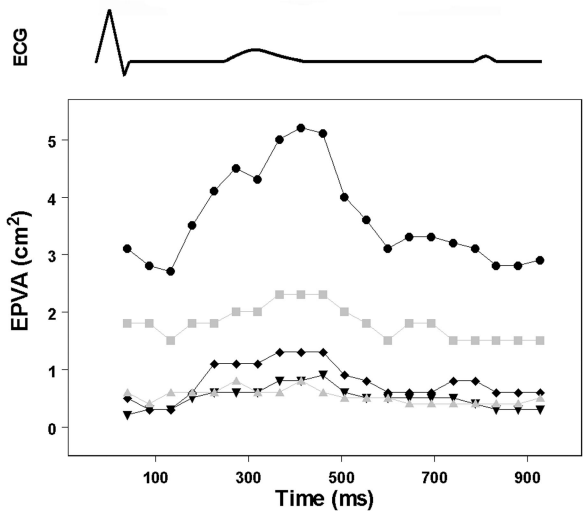

Fig. 5. Plot of the EPVA throughout the cardiac cycle for one subject. Measurements of each vein as well as their sum are shown. Note that each vein displays a similar pattern as a function of time but do not all peak simultaneously. Also of significance is that the change in area for each vein is rather minor but, when combined, results in a substantial total EPVA variation. The ECG displayed is a schematic and serves as an aid to clarify timing within the cardiac cycle. See text for details. Shaded squares, right superior pulmonary vein; solid diamonds, left superior pulmonary vein; shaded triangles, left inferior pulmonary vein; solid inverted triangles, right inferior pulmonary vein; solid circles, sum of all four pulmonary vein areas.

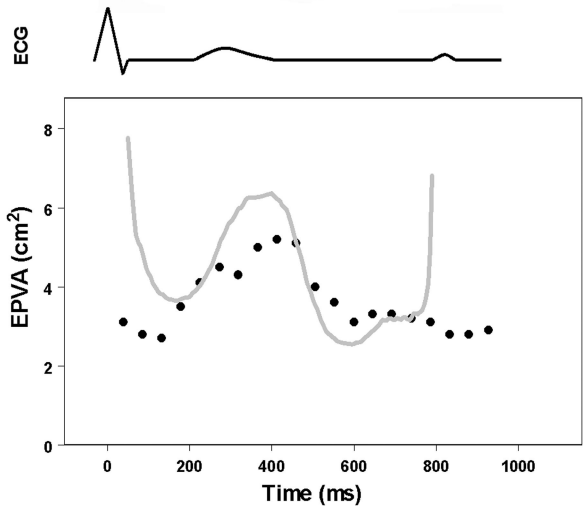

Fig. 6. Plot of predicted EPVA via *Eq. 7* (shaded line) superimposed on measured combined EPVA from MRI (solid circles) for one subject. Values of predicted EPVA from *Eq. 7* approaching infinity resulting from very small denominators were omitted for clarity. Note the similarity between the two curves, particularly near end systole. The ECG displayed is a schematic and serves as an aid to clarify timing within the cardiac cycle. See text for details.

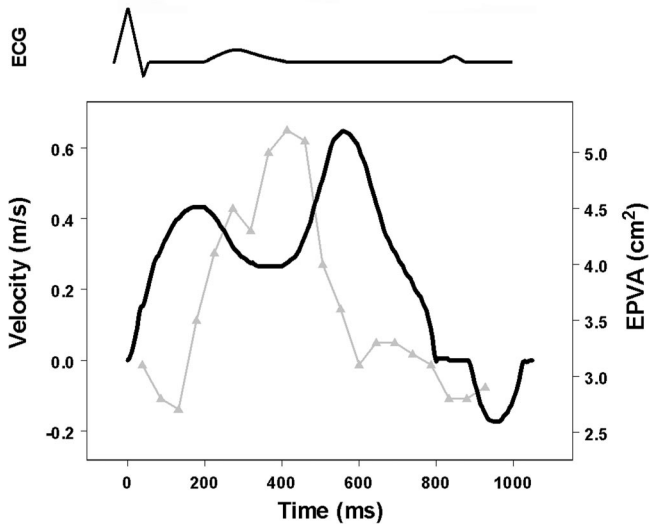

Fig. 7. Plot of the echocardiographically measured pulmonary vein flow velocity contour (solid line, *left* vertical axis) superimposed with the MRI-measured EPVA scaled appropriately (shaded triangles, *right* vertical axis) for one subject. Note how the EPVA peaks near a relative minimum of pulmonary vein flow at end systole. The ECG displayed is a schematic and serves as an aid to clarify timing within the cardiac cycle. See text for details.

acquired via cardiac MRI and echocardiography directly led to the prediction and in vivo validation of time-varying EMVA (2) and EPVA.

Interestingly, maximum EPVA consistently precedes maximum flow through the PVs (Fig. 7). Because our earlier findings of time-varying EMVA indicated that the EMVA curve corresponded in time with the transmitral flow profile reasonably well (2), the fundamental explanation for the change in EPVA must differ from the explanation for time-varying EMVA. The mitral valve effectively acts as windsock: the faster blood flows through it, the wider (in general) the leaflets separate; hence, flow velocity and EMVA are nearly perfectly aligned in time (phase). In contrast, the mechanism driving EPVA change is more subtle yet easily understood on kinematic grounds when considering the LA volume curve as function of time and how the tissue (atrial walls + mitral annulus) moves (see *animation 2*, http://ajpheart.physiology.org/cgi/content/full/00713.2004/DC1). Driven by ventricular systole, the mitral annulus (with closed leaflets) is drawn toward the ventricular apex, the mediastinal aspect of the atrium remains fixed (although it is free to slide along the pericardial surface), the lateral wall of the atrium slides along the pericardial sack, and the atrium acts as an aspiration pump. Thus, during ventricular systole, the atrial tissue, including the PV ostia, relaxes and is stretched by the apically directed motion of the annulus. Consequently, normal LA volume more than doubles, and in some cases triples, as the ventricle ejects (3, 4, 16, 17). Such volume changes of the entire LA chamber mandate that the normal, relaxed LA tissue be compliant while it is stretched (27), a statement consistent with results showing that LA compliance increases with surgical removal of the pericardium (14). Because the origins of the PVs are, in fact, atrial (myocardial) tissue (13), it is reasonable for the EPVA to be compliant (stretched) in a manner similar to the LA as a whole, and this facilitates the substantial increase in LA volume during ventricular systole (via the Doppler PV S-wave). Tissue compliance and mechanical (base to apex) displacement of atrial tissue by ventricular systole explain the remarkable similarity between the LA volume curve and measured EPVA curve in our data (Fig. 8). Therefore, whereas changes in EMVA are governed primarily by flow through the mitral valve, changes in EPVA are governed by the time-varying LA volume itself.

It is also important to point out that because PV flow in early diastole (corresponding to mitral valve opening and the acceleration portion of the echocardiographic PV D wave) travels directly to the LV via the LA conduit volume (4), maximizing EPVA at or near the beginning of diastole clearly facilitates optimization of early rapid LV filling. Similarly, during atrial contraction, LV filling would also be optimized if the EPVA became smaller to minimize retrograde flow back into the PVs. A recent study (13) has demonstrated that atrial myocardial fibers extend into the PVs and include fibers that are oriented circumferentially. Accordingly, we noticed in 9 of 10 subjects (data not shown) that total EPVA in late diastasis (immediately before atrial contraction) was greater than EPVA at end diastole (immediately after atrial contraction), supporting the idea that atrial contraction constricts the PV orifice like a sphincter, directing blood primarily to the LV and minimizing retrograde flow (see *animation 1* for an example from one vein). Further studies focused on the role of the PV ostia as a flow rectifier specifically during atrial contraction are warranted.

Recently, PV assessment has become significant, particularly in the fields of cardiac surgery and electrophysiology in the treatment protocols for atrial fibrillation. It has been widely supported that one of the common side effects of treating atrial fibrillation using radiofrequency catheter ablation of LA tissue is stenosis of one or more PVs, and evidence of such stenoses has been documented via both echocardiography and cardiac MRI (6, 9, 15, 24, 33, 34). However, no such study to our knowledge has discussed the particular impact of PV stenosis after these procedures in the setting of PVs with time-varying

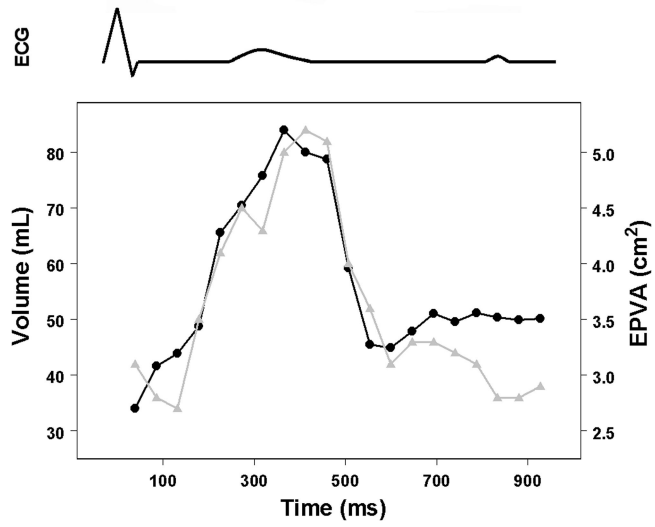

Fig. 8. Plot of the MRI-measured LA volume curve (solid circles, *left* vertical axis) superimposed with the MRI-measured total EPVA scaled appropriately (shaded triangles, *right* vertical axis) for one subject. Note the similarity of the two curves, particularly in late systole and early diastole. The ECG displayed is a schematic and serves as an aid to clarify timing within the cardiac cycle. See text for details.

areas. It is unknown whether the area of a stenotic vein still varies in a cardiac cycle-dependent manner to the same extent as a normal vein or whether the stenosis leads to a less compliant, more rigid EPVA, which would impact filling of both the LA and LV [via the LA conduit volume in early diastole (4)]. Future studies addressing the effect of PV stenosis on the variation of EPVA throughout the cardiac cycle are therefore warranted.

Limitations. Limitations in MRI imaging method and the synchronization of the MRI and echocardiographic data have been discussed previously (2–4). However, we feel it prudent to mention that the temporal resolution of the MRI scans ranged from ~30 to 50 ms, corresponding to a frame rate of 20–33 frames/s. Although faster frame rates are achievable using other MRI imaging protocols, this rate was selected to balance the simultaneous needs of subject comfort, breathhold duration, scan duration, and spatial resolution. Additionally, because the MRI volumetric data were acquired using 9-mm-thick slices, there is the possibility of systematic error in the volumes reported in this study. However, the technique employed in this study is the current MRI research standard. Manual tracings of the chambers may also raise concern, but it has also been the standard approach for chamber volume determination and has agreed well with a recently developed automated method (30).

Because the MRI scan and echocardiographic study were contemporaneous but not simultaneous, we could not assure the maintenance of an absolutely constant heart rate in our subjects. Because the MRI imaging involved frequent breathholds, the measured heart rate of some subjects was found to be higher during the MRI scan than during the echocardiographic study (from around 60–80 beats/min). However, during such minor changes in heart rate, the change in duration of systole is minimal, and the change in duration of diastolic early rapid filling is similarly minimal (7). We also note that the timing of events during systole and early diastole was consistent between the echocardiographic measurements and the MRI measurements even when the heart rates of subjects varied somewhat between the two studies.

It is not surprising that the predicted EPVA did not better match the measured EPVA from the short-axis MRI data. Limitations of transthoracic PV echocardiographic imaging have been well characterized (21, 28). Frequently, only one vein may be imaged clearly. Previous studies using both echocardiography and MRI have demonstrated that flow through the four PVs can vary because different veins can exhibit different flow contours (5, 8, 10). This, in part, may account for the discrepancies between predicted and measured EPVA curves as well as between LA volume curves calculated via Marino's method and those measured directly with MRI (see Fig. 4). However, imaging of the PV with transthoracic echocardiography is a common practice, and it should be noted how accurate the predicted EPVA curve is given this limitation. Hence, assuming the flow contour is representative of all veins is a reasonable first approximation.

Because we measured EPVA using only the short-axis MRI data, it may appear that our findings of time-varying EPVA could be the result of the veins moving in and out of the imaging plane throughout the cardiac cycle. We are assured that this is not the case. Because our short-axis data slices have no gap between them, if the veins moved from one plane to another during the cardiac cycle, we would observe it, and we did not. Also, in some of the studies, PV flow was imaged using a cross-sectional approach to the veins. It was noted in this view that the origins of the veins remained fixed in the mediastinum throughout the cardiac cycle (data not shown). This raises the question of whether a cross-sectional imaging plane would be better suited for measuring the changing PV areas. Because the data for the image are acquired and averaged from the entire thickness of the image plane (in this case, 8–10 mm), the segment of the PV that varies in area would be averaged in with either the nonoscillatory segment of the vein or the LA itself, depending on the precise location of the imaging plane. The time-varying nature of the PV ostia, therefore, is unlikely to be detectable in the cross-sectional view.

In conclusion, EPVA varies as a function of time throughout the cardiac cycle. The pattern of observed EPVA variation makes physiological sense in that its behavior is in phase with the variation of LA volume, indicating that the expansion of the compliant LA, driven by ventricular systole, causes simultaneous enlargement of EPVA and facilitates LA filling during the Doppler PV S wave. Consequently, the PVAs are maximal at or near end systole, and this also facilitates the rapid filling of the LV via the LA conduit volume and the PV D wave in early diastole. Moreover, the observed variation in EPVA helps explain differences between LA volume curves estimated via Marino's echocardiographic method and those measured via cardiac MRI. Modification and/or disruption of the time-varying EPVA in hearts undergoing the procedures in the treatment of atrial fibrillation are unknown and merit future study.

ACKNOWLEDGMENTS

The authors thank Shelton Caruthers for technical direction, Mary Watkins and Todd Williams for MRI image acquisition, and Peggy Brown for expert echocardiographic image acquisition.

GRANTS

This study was supported in part by the Heartland Affiliate of the American Heart Association (Dallas, TX), the Whitaker Foundation (Roslyn VA), National Heart, Lung, and Blood Institute Grants HL-54179 and HL-04023 (Bethesda MD), the Alan A. and Edith L. Wolff Charitable Trust (St. Louis, MO), and Philips Medical Systems (Best, The Netherlands).

REFERENCES

1. **Appleton CP, Galloway JM, Gonzalez MS, Gaballa M, and Basnight MA.** Estimation of left ventricular filling pressures using two-dimensional and Doppler echocardiography in adult patients with cardiac disease. Additional value of analyzing left atrial size, left atrial ejection fraction and the difference in duration of pulmonary venous and mitral flow velocity at atrial contraction. *J Am Coll Cardiol* 22: 1972–1982, 1993.
2. **Bowman AW, Frihauf PA, and Kovács SJ.** The time-varying effective mitral valve area: prediction and validation using cardiac MRI and Doppler echocardiography in normal subjects. *Am J Physiol Heart Circ Physiol* 287: H1650–H1657, 2004.
3. **Bowman AW and Kovács SJ.** Assessment and consequences of the constant-volume attribute of the four-chambered heart. *Am J Physiol Heart Circ Physiol* 285: H2027–H2033, 2003.
4. **Bowman AW and Kovács SJ.** Left atrial conduit volume is generated by deviation from the constant-volume state of the left heart: a combined MRI-echocardiographic study. *Am J Physiol Heart Circ Physiol* 286: H2416–H2424, 2004.
5. **Carlsson M, Cain P, Holmqvist C, Stahlberg F, Lundback S, and Arheden H.** Total heart volume variation throughout the cardiac cycle in man. *Am J Physiol Heart Circ Physiol* 287: H243–H250, 2004.
6. **Chen SA, Hsieh MH, Tai CT, Tsai CF, Prakash VS, Yu WC, Hsu TL, Ding YA, and Chang MS.** Initiation of atrial fibrillation by ectopic beats originating from the pulmonary veins: electrophysiological characteristics,

pharmacological responses, and effects of radiofrequency ablation. *Circulation* 100: 1879–1886, 1999.
7. **Chung CS, Karamanoglu M, and Kovács SJ.** The duration of diastole and its phases as a function of heart rate during supine bicycle exercise. *Am J Physiol Heart Circ Physiol* 287: H2003–H2008, 2004. First published June 24, 2004; doi:10.1152/ajpheart.00404.2004.
8. **De Marchi SF, Bodenmuller M, Lai DL, and Seiler C.** Pulmonary venous flow velocity patterns in 404 individuals without cardiovascular disease. *Heart* 85: 23–29, 2001.
9. **Dill T, Neumann T, Ekinci O, Breidenbach C, John A, Erdogan A, Bachmann G, Hamm CW, and Pitschner HF.** Pulmonary vein diameter reduction after radiofrequency catheter ablation for paroxysmal atrial fibrillation evaluated by contrast-enhanced three-dimensional magnetic resonance imaging. *Circulation* 107: 845–850, 2003.
10. **Fyrenius A, Wigstrom L, Ebbers T, Karlsson M, Engvall J, and Bolger AF.** Three dimensional flow in the human left atrium. *Heart* 86: 448–455, 2001.
11. **Hall AF, Aronovitz JA, Nudelman SP, and Kovács SJ.** Automated method for characterization of diastolic transmitral Doppler velocity contours: late atrial filling. *Ultrasound Med Biol* 20: 859–869, 1994.
12. **Hall AF and Kovács SJ.** Automated method for characterization of diastolic transmitral Doppler velocity contours: early rapid filling. *Ultrasound Med Biol* 20: 107–116, 1994.
13. **Hassink RJ, Aretz HT, Ruskin J, and Keane D.** Morphology of atrial myocardium in human pulmonary veins: a postmortem analysis in patients with and without atrial fibrillation. *J Am Coll Cardiol* 42: 1108–1114, 2003.
14. **Hoit BD, Shao Y, Gabel M, and Walsh RA.** Influence of pericardium on left atrial compliance and pulmonary venous flow. *Am J Physiol Heart Circ Physiol* 264: H1781–H1787, 1993.
15. **Jais P, Weerasooriya R, Shah DC, Hocini M, Macle L, Choi KJ, Scavee C, Haissaguerre M, and Clementy J.** Ablation therapy for atrial fibrillation (AF): past, present and future. *Cardiovasc Res* 54: 337–346, 2002.
16. **Jarvinen V, Kupari M, Hekali P, and Poutanen VP.** Assessment of left atrial volumes and phasic function using cine magnetic resonance imaging in normal subjects. *Am J Cardiol* 73: 1135–1138, 1994.
17. **Jarvinen VM, Kupari MM, Poutanen VP, and Hekali PE.** A simplified method for the determination of left atrial size and function using cine magnetic resonance imaging. *Magn Reson Imaging* 14: 215–226, 1996.
18. **Kovács SJ Jr, Barzilai B, and Pérez JE.** Evaluation of diastolic function with Doppler echocardiography: the PDF formalism. *Am J Physiol Heart Circ Physiol* 252: H178–H187, 1987.
19. **Marino P, Destro G, Barbieri E, and Zardini P.** Early left ventricular filling: an approach to its multifactorial nature using a combined hemodynamic-Doppler technique. *Am Heart J* 122: 132–141, 1991.
20. **Marino P, Prioli AM, Destro G, LoSchiavo I, Golia G, and Zardini P.** The left atrial volume curve can be assessed from pulmonary vein and mitral valve velocity tracings. *Am Heart J* 127: 886–898, 1994.
21. **Naqvi TZ.** Diastolic function assessment incorporating new techniques in Doppler echocardiography. *Rev Cardiovasc Med* 4: 81–99, 2003.
22. **Pagel PS, Kehl F, Gare M, Hettrick DA, Kersten JR, and Warltier DC.** Mechanical function of the left atrium: new insights based on analysis of pressure-volume relations and Doppler echocardiography. *Anesthesiology* 98: 975–994, 2003.
23. **Rodevand O, Bjornerheim R, Ljosland M, Maehle J, Smith HJ, and Ihlen H.** Left atrial volumes assessed by three- and two-dimensional echocardiography compared to MRI estimates. *Int J Card Imaging* 15: 397–410, 1999.
24. **Schwartzman D, Kanzaki H, Bazaz R, and Gorcsan J III.** Impact of catheter ablation on pulmonary vein morphology and mechanical function. *J Cardiovasc Electrophysiol* 15: 161–167, 2004.
25. **Shiller NB, Shah PM, Crawford M, DeMaria A, Devereux R, Feigenbaum H, Gutesell H, Reichek N, Sahn D, Schnittger I, Silberman NH, and Tajik AJ.** Recommendations for quantitation of the left ventricle by two-dimensional echocardiography. American Society of Echocardiography Committee on Standards, Subcommittee on Quantitation of Two-Dimensional Echocardiograms. *J Am Soc Echocardiogr* 2: 358–367, 1989.
26. **Stefanadis C, Dernellis J, and Toutouzas P.** A clinical appraisal of left atrial function. *Eur Heart J* 22: 22–36, 2001.
27. **Suga H.** Importance of atrial compliance in cardiac performance. *Circ Res* 35: 39–43, 1974.
28. **Tabata T, Thomas JD, and Klein AL.** Pulmonary venous flow by Doppler echocardiography: revisited 12 years later. *J Am Coll Cardiol* 41: 1243–1250, 2003.
29. **Tsang TS, Barnes ME, Gersh BJ, Bailey KR, and Seward JB.** Left atrial volume as a morphophysiologic expression of left ventricular diastolic dysfunction and relation to cardiovascular risk burden. *Am J Cardiol* 90: 1284–1289, 2002.
30. **Tseng WYI, Liao TY, and Wang JL.** Normal systolic and diastolic functions of the left ventricle and left atrium by cine magnetic resonance imaging. *J Cardiovasc Magn Reson* 4: 443–457, 2002.
31. **Van der Geest RJ and Reiber JH.** Quantification in cardiac MRI. *J Magn Reson Imaging* 10: 602–608, 1999.
32. **Wittkampf FH, Vonken EJ, Derksen R, Loh P, Velthuis B, Wever EF, Boersma LV, Rensing BJ, and Cramer MJ.** Pulmonary vein ostium geometry: analysis by magnetic resonance angiography. *Circulation* 107: 21–23, 2003.
33. **Yang M, Akbari H, Reddy GP, and Higgins CB.** Identification of pulmonary vein stenosis after radiofrequency ablation for atrial fibrillation using MRI. *J Comput Assist Tomogr* 25: 34–35, 2001.
34. **Yu WC, Hsu TL, Tai CT, Tsai CF, Hsieh MH, Lin WS, Lin YK, Tsao HM, Ding YA, Chang MS, and Chen SA.** Acquired pulmonary vein stenosis after radiofrequency catheter ablation of paroxysmal atrial fibrillation. *J Cardiovasc Electrophysiol* 12: 887–892, 2001.